

Collective behavior of independent scaled Brownian particles with renewal resetting

Ohad Vilk^a, Baruch Meerson^a

^a*Racah Institute of Physics, Hebrew University of Jerusalem, Jerusalem, 91904, Israel*

Abstract

We study collective dynamics of an ensemble of $N \gg 1$ independent particles undergoing anomalous diffusion with random renewal resetting. The anomalous diffusion is modeled by the scaled Brownian motion (sBm): a Gaussian process, characterized by a power-law time dependence of the diffusion coefficient, $D(t) \sim t^{2H}$, where $H > 0$. The particles independently reset to the origin, and each particle's clock is set to zero upon spatial resetting. Employing the known steady-state position distribution of a *single* particle undergoing the sBm with renewal resetting [Bodrova et al., Phys. Rev. E **100**, 012120 (2019)], we study the collective dynamics of N particles. We determine the statistics of the system radius ℓ . The typical fluctuations of ℓ fall under the Gumbel universality class, and we use extreme value statistics to calculate the moments of ℓ . We also study the large-deviation statistics of the center of mass (COM), where for $H > 1/2$ we uncover an anomalous scaling behavior of the COM distribution, and a singularity in the corresponding rate function, due to a “big jump” effect.

Keywords: Stochastic resetting, Anomalous diffusion, Scaled Brownian motion, Non-equilibrium steady states, Extreme value statistics, Big jump principle

1. Introduction

Stochastic resetting represents a large class of stochastic processes where a random motion is instantaneously terminated at random times and restarted

Email addresses: ohad.vilk@mail.huji.ac.il (Ohad Vilk),
meerson@mail.huji.ac.il (Baruch Meerson)

from a specified location [1]. This paradigm turns out to be highly relevant to a broad range of natural processes and applications [2–6]. It is not surprising, therefore, that since its introduction in 2011 by Evans and Majumdar [7], stochastic resetting has attracted significant and sustained attention. The problem becomes even richer and more interesting when there are many resetting agents, see Ref. [8] for a review.

Stochastic resetting models differ among themselves by the nature of the random motion between the resetting events. Here we are interested in multi-particle systems such that, between the resetting events, the particles exhibit *anomalous diffusion*, where the mean squared displacement of a particle scales with time as t^{2H} [9–11]. The regime $0 < H < 1/2$ describes subdiffusion, while the regime $H > 1/2$ corresponds to superdiffusion, which, for $H > 1$, becomes super-ballistic. Standard diffusion is recovered at $H = 1/2$. Anomalous transport with stochastic resetting has been studied in continuous-time random walks, scaled Brownian motion, and other anomalous diffusion processes [12–17]. A simple way to model anomalous diffusion, that we adopt here, is scaled Brownian motion (sBm): a Gaussian process with independent increments, characterized by a power-law dependence of the diffusion coefficient on time, $D(t) \sim t^{2H}$, where H can be any positive number [18–20].

Stochastic resetting can be added to sBm in two different ways [15, 14]. In the first one – the nonrenewal resetting – the spatial resetting events do not affect the time-dependence of the diffusion coefficient: the particle does not forget its local time [15]. In the second one – the renewal resetting – the local clock of the particle is reset to zero upon the particle’s spatial resetting [14]. The differences between these two settings have been thoroughly discussed in Refs. [14, 15]. In particular, for the nonrenewal case the probability distribution of the particle position remains non-stationary at all times. In contrast, under renewal resetting the position distribution reaches a nonequilibrium steady state whose tails are stretched or compressed exponentials (see below). In this work we study the latter case and focus on the collective properties of $N \gg 1$ independent scaled Brownian particles subject to renewal resetting.

Here are the main results of this work. Employing the known steady-state position distribution of a *single* particle undergoing sBm with renewal resetting [14], we determine the full statistics of the system’s radius ℓ and of the center of mass (COM). We show that the typical fluctuations of the system radius, defined as the maximum distance of a particle from the origin,

fall within the Gumbel universality class for all $H > 0$. In contrast, the large deviations of the COM behaves very differently for $H < 1/2$ and $H > 1/2$. Remarkably, for $H > 1/2$ the COM large-deviation statistics exhibit anomalous scaling behavior and a singularity (a jump in the first derivative) in the associated large deviation function. These features are caused by a “big-jump” mechanism, where a single particle wanders far from the rest of the particles and dominates the statistics.

Here is a plan of the remainder of the paper. In Sec. 2 we define the microscopic dynamics of the model. In Secs. 3 and 4 we determine the complete statistics of the radius and of the COM of the system. Finally, in Sec. 5 we summarize our results and discuss a promising direction for future work. Throughout the paper we compare our results with Monte-Carlo simulations.

2. Microscopic Model

We consider $N \gg 1$ independent particles moving on the real line. Each particle performs the sBm [18–20] with exponent $H > 0$ and diffusion coefficient D :

$$\langle [x_i(t) - x_i(s)]^2 \rangle = 2D |t - s|^{2H}, \quad i = 1, \dots, N. \quad (1)$$

At random times one particle is randomly chosen with Poisson rate Nr and reset to the origin. The particle’s clock is also reset to zero, and the particle resumes the sBm. The single-particle ($N = 1$) variant of this model was introduced and analyzed by Bodrova et al. [14].

At times much longer than $1/r$ this ensemble of particles reaches a nonequilibrium steady state (NESS), and our objective is to characterize this NESS. To this end we will calculate the probability distributions of the system’s radius ℓ and of the systems’ COM. Since the particles are non-interacting, these two distributions are completely determined by the steady-state position distribution $p_s(x)$ in the single-particle case, $N = 1$. The latter distribution was calculated by Bodrova et al. [14], and it reads:

$$p_s(x) = \frac{1}{\sqrt{4\pi}} \int_0^\infty d\tau \frac{e^{-\frac{x^2}{4\tau^{2H}} - \tau}}{\tau^H}. \quad (2)$$

Here, and quite often in the following, we set $r = D = 1$. This corresponds to a proper choice of units of distance, \sqrt{D}/r^H , and time, $1/r$.

The integral in Eq. (2) does not allow a convenient exact evaluation. However, as we will see shortly, the most important properties of the two statistics, that we are going to focus on, are determined by the large- $|x|$ tail of $p_s(x)$. This tail can be determined via a saddle-point evaluation of the integral in Eq. (2), and one obtains [14, 21]

$$p_s(|x| \gg 1) \simeq \left(\frac{H}{2}\right)^{\frac{1-2H}{2(2H+1)}} \frac{|x|^{\frac{1-2H}{2H+1}}}{\sqrt{2(2H+1)}} \exp \left[-\frac{(2H+1) \left(\frac{H}{2}\right)^{\frac{1}{2H+1}} |x|^{\frac{2}{2H+1}}}{2H} \right]. \quad (3)$$

This tail is super-exponential for $H < 1/2$ and sub-exponential for $H > 1/2$. In the marginal case of the standard Brownian motion, $H = 1/2$, the tail is exponential and coincides with the exact single-particle steady-state distribution $p_s(x) = (1/2) e^{-|x|}$ [7].

For reference purposes, we also present the $|x| \ll \ell$ asymptotics of $p_s(x)$ [21]

$$p_s(|x| \ll \ell_0) \simeq \frac{1}{\sqrt{4\pi}} \times \begin{cases} \Gamma(1-H) - \Gamma(1-3H) \frac{x^2}{4}, & \text{for } 0 < H < 1/3, \\ \Gamma(1-H) + \frac{1}{2H} \Gamma\left(\frac{1}{2} - \frac{1}{2H}\right) \left(\frac{x^2}{4}\right)^{\frac{1-H}{2H}}, & \text{for } 1/3 < H < 1, \\ \frac{1}{2H} \Gamma\left(\frac{1}{2} - \frac{1}{2H}\right) \left(\frac{x^2}{4}\right)^{\frac{1-H}{2H}}, & \text{for } H > 1. \end{cases} \quad (4)$$

The maximum density is observed at $x = 0$, and it is finite only for $H < 1$. For $H \geq 1$ it diverges, but this singularity is integrable.

3. Full statistics of the system radius ℓ

To determine the full statistics of the system's radius ℓ , we integrate the single-particle distribution $p_s(x)$ in Eq. (2) over $x \in [-\ell, \ell]$ and arrive at the cumulative single-particle probability

$$I(\ell) = \int_0^\infty e^{-\tau} \operatorname{erf}\left(\frac{\ell}{2}\tau^{-H}\right) d\tau. \quad (5)$$

Since the particles are independent, the cumulative probability that the system radius does not exceed ℓ can be written as

$$F_N(\ell) = [I(\ell)]^N. \quad (6)$$

Differentiating this expression with respect to ℓ , we obtain the exact probability density of the radius ℓ :

$$f_N(\ell) = N I'_\ell(\ell) [I(\ell)]^{N-1}, \quad (7)$$

where,

$$I'_\ell(\ell) = \frac{1}{\sqrt{\pi}} \int_0^\infty \tau^{-H} \exp\left(-\tau - \frac{\ell^2}{4}\tau^{-2H}\right) d\tau. \quad (8)$$

Fig. 1 shows numerically evaluated $f_N(\ell)$ alongside with our simulation result for different H ¹.

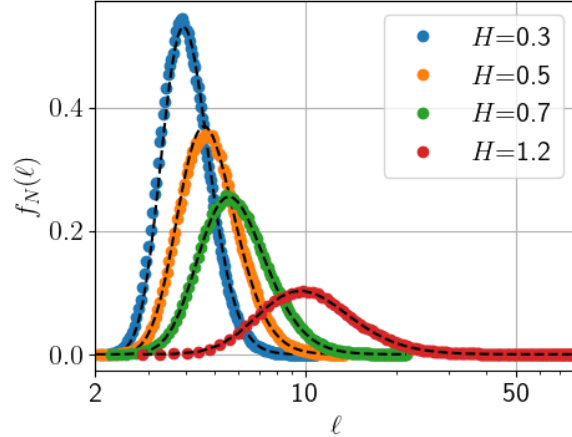


Figure 1: Steady-state distribution of the system radius ℓ for different values of H (see legend). Lines: Eq. (7), evaluated numerically. Symbols: simulations, where $N = 100$, and the simulation time is $t = 10^5$.

The average radius $\bar{\ell}$ is given by the first moment of $f_N(\ell)$:

$$\bar{\ell} = \int_0^\infty \ell f_N(\ell) d\ell = \int_0^\infty [1 - F_N(\ell)] d\ell = \int_0^\infty [1 - I(\ell)^N] d\ell, \quad (9)$$

¹We simulate N particles, where resets occur at a Poissonian rate rN with a randomly chosen particle reset to zero, and between reset events particle increments are Gaussian with variance $2D_{\text{eff},i} dt$. Notably, the system relaxes on a timescale $\mathcal{O}(1/r)$, so simulations up to time 10^5 provide approximately 10^5 effectively uncorrelated samples, see Ref. [21] for more details.

where we have integrated by parts and used Eq. (6). For the standard Brownian motion, $H = 1/2$, Eq. (9) yields $I(\ell) = 1 - e^{-\ell}$, and we obtain

$$\bar{\ell} = \int_0^\infty [1 - (1 - e^{-\ell})^N] d\ell = H_N = \psi(N + 1) + \gamma, \quad (10)$$

in agreement with Ref. [22]. Here H_N is the N -th harmonic number, $\psi(\dots)$ is the digamma function, and $\gamma = 0.57721\dots$ is Euler's constant.

For general $H > 0$ the integral in Eq. (9) is hard to evaluate analytically. Fortunately, there is an important shortcut here, based on the observation that the cumulative distribution $F_N(\ell) = I(\ell)^N$ is the distribution of the maximum of N independent random numbers drawn from the same parent distribution $I(\ell)$. Therefore, we can apply to this case the well-developed theory of extreme-value statistics (EVS) of identically-distributed independent random numbers [23–26], see Ref. [27] for an accessible exposition. According to the EVS theory, at $N \gg 1$ the average steady-state radius $\bar{\ell}$ is completely determined by the *tail* of the parent distribution $I(\ell)$. Once the tail is known, the EVS theory provides both the leading-order result for $\bar{\ell}$ and its universal subleading correction [27]. Our task therefore reduces to obtaining the large- ℓ asymptotic behavior of the “survival function”

$$1 - I(\ell) = \int_0^\infty e^{-\tau} \operatorname{erfc}\left(\frac{\ell\tau^{-H}}{2}\right) d\tau. \quad (11)$$

Using the identity

$$\operatorname{erfc}(z) = \frac{2}{\sqrt{\pi}} \int_z^\infty e^{-s^2} ds,$$

and noting that the integrand in Eq. (11) is strictly positive, we can exchange the order of integration (even though the inner integration limits depend on τ). We obtain

$$\begin{aligned} 1 - I(\ell) &= \frac{2}{\sqrt{\pi}} \int_0^\infty \int_{\frac{\ell}{2}\tau^{-H}}^\infty e^{-\tau} e^{-s^2} ds d\tau \\ &= \frac{2}{\sqrt{\pi}} \int_0^\infty e^{-s^2} \left[\int_{(\ell/2s)^{1/H}}^\infty e^{-\tau} d\tau \right] ds = \frac{2}{\sqrt{\pi}} \int_0^\infty e^{-\Psi(s, \ell)} ds, \end{aligned} \quad (12)$$

where

$$\Psi(s, \ell) = s^2 + \left(\frac{\ell}{2}\right)^{1/H} s^{-1/H}.$$

Since we are interested in the $\ell \gg 1$ asymptotic, we can apply the saddle point method and obtain

$$1 - I(\ell) \simeq C_H \exp(-\kappa_H \ell^{\frac{2}{2H+1}}), \quad (13)$$

where

$$C_H = \frac{2\sqrt{H}}{\sqrt{2H+1}} \quad \text{and} \quad \kappa_H = 2^{-\frac{2(H+1)}{2H+1}} H^{-\frac{2H}{2H+1}} (2H+1). \quad (14)$$

As one can see from Eq. (13), the $\ell \rightarrow \infty$ tail of the survival function $1 - I(\ell)$ decays faster than a power law for all $H > 0$. Therefore, according to the EVS theory [27], the typical fluctuations of ℓ belong to the Gumbel universality class. That is, after proper centering and rescaling, the typical fluctuations are distributed, as $N \rightarrow \infty$, as follows:

$$\Pr\left(\frac{\ell - b_N}{a_N} \leq z\right) \rightarrow e^{-e^{-z}},$$

with the mean

$$b_N \simeq \kappa_H^{-\frac{2H+1}{2}} [\ln(C_H N)]^{\frac{2H+1}{2}}. \quad (15)$$

The local scale of fluctuations around b_N is determined by the inverse of the "hazard rate" $h(\ell) = I'(\ell)/[1 - I(\ell)]$, giving

$$a_N \simeq \frac{2H+1}{2 \kappa_H^{\frac{2H+1}{2}}} [\ln(C_H N)]^{H-1/2}. \quad (16)$$

Consequently, the average radius $\bar{\ell}$ has the following universal $N \rightarrow \infty$ asymptotic form:

$$\bar{\ell} \simeq b_N + \gamma a_N = \kappa_H^{-\frac{2H+1}{2}} [\ln(C_H N)]^{H+1/2} + \gamma \frac{2H+1}{2 \kappa_H^{\frac{2H+1}{2}}} [\ln(C_H N)]^{H-1/2}. \quad (17)$$

Notably, the first term in Eq. (17) b_n represents the most probable system radius, while the second term γa_N describes a universal correction originating from the Gumbel statistics. Note that for $0 < H < 1/2$, the second term decreases with an increase of N so that the average radius is equal to b_n without any correction which survives the limit of $N \rightarrow \infty$. In contrast, when $H > 1/2$, the second term *increases* with N , although slower than the

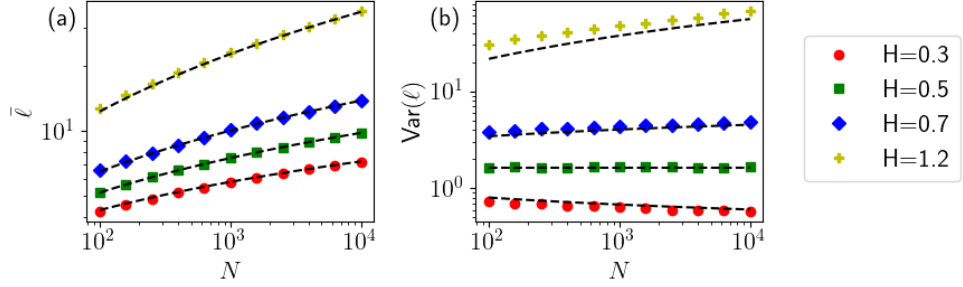


Figure 2: (a) The average system radius $\bar{\ell}$, Eq. (17) and (b) the variance of the system radius, Eq. (18), vs. N for different values of H (see legend). Lines: theoretical predictions. Symbols: simulation results, where the simulation time is $t = 10^5$.

first term. For the marginal value $H = 1/2$ the second term is constant $O(1)$, and we obtain $C_{1/2} = \kappa_{1/2} = 1$, and $\bar{\ell} \simeq \ln N + \gamma$, in agreement with Ref. [22] and with the large- N limit of Eq. (10).

Using the EVS, we can also calculate higher moments of ℓ . In particular, the variance is

$$\text{Var}(\ell) = \frac{\pi^2}{6} a_N^2 + o(a_N^2) \simeq \frac{\pi^2}{6} \frac{(2H+1)^2}{4 \kappa_H^{2H+1}} \ln(C_H N)]^{2H-1}. \quad (18)$$

For $H = 1/2$ this gives $\text{Var}(\ell) = \pi^2/6$, again in agreement with Ref. [22]. In Fig. 2 we compare Eqs. (17) and (18) with our numerical simulations for different H .

4. Full statistics of the center of mass

Now we consider the probability distribution $P(a, N)$ of observing the center of mass of the system in the steady state,

$$\bar{x} \equiv \frac{1}{N} \sum_{i=1}^N x_i, \quad (19)$$

to be equal to a prescribed value a . Sometimes it will be more convenient to deal with the probability distribution $\mathcal{P}(A, N)$ of the sum itself,

$$\Sigma \equiv \sum_{i=1}^N x_i = A. \quad (20)$$

Since the particles are non-interacting, Σ is a sum of $N \gg 1$ independent identically distributed random numbers. Similarly to the statistics of ℓ , the statistics of Σ is strongly affected by the behavior of the large- $|x|$ tail of the “parent distribution” $p_s(x)$ [28–30]. As follows from Eq. (3), there are two qualitatively different regimes of the scaling behavior of the probability distributions $P(a, N)$ and $\mathcal{P}(\Sigma, N)$, depending on H .

For $H \leq 1/2$ the large- $|x|$ tail of $p_s(x)$ falls off exponentially, or faster than exponentially, with $|x|$, see Eq. (3). This regime corresponds to the “standard” large-deviation scaling behavior of $\mathcal{P}(A, N)$ at $N \rightarrow \infty$ [28],

$$-\ln \mathcal{P}(A, N) \simeq N f\left(\frac{A}{N}\right) \equiv N f(a), \quad (21)$$

where the rate function $f(a)$ remains analytic even in the limit of $N \rightarrow \infty$.

For $H > 1/2$ the large- $|x|$ tail of $p_s(x)$ decays as a stretched exponential, see Eq. (3). This leads to an anomalous scaling behavior of the large deviations [28–31]:

$$-\ln \mathcal{P}(A, N) \simeq N^\mu \phi\left(\frac{A}{N^\nu}\right), \quad (22)$$

where the anomalous exponents $\mu > 0$ and $\nu > 0$ are smaller than 1. The underlying mechanism of the scaling anomaly is the “big jump effect” observed at sufficiently large A , where a rare large deviation of the coordinate of a *single* particle – the big jump – provides a dominant contribution to A and determines its statistics. Remarkably, in the limit of $N \rightarrow \infty$ while $A/N^\nu = \text{const}$, the rate function $\phi(y)$ exhibits a finite jump in its first derivative at some point y_c . Such a nonanalyticity is usually interpreted as a dynamical phase transition of first order, see e.g. [32]. Below the transition point $A = A_c$ all the particles give comparable contributions to A , and the fluctuations of A are Gaussian, whereas above the transition point the rate function is affected by the big jump. An important attribute of this scenario is the regime of moderately large deviations at $A \gtrsim A_c$, where the two mechanisms – the Gaussian fluctuations and the big jump – coexist, and the resulting rate function $\phi(\dots)$ is determined by their competition.

Below we consider the standard scaling regime $H \leq 1/2$ and the anomalous scaling regime $H > 1/2$ separately. Prior to that, however, let us determine the variance of the distributions $P(a, N)$ and $\mathcal{P}(A)$. The variance of the position of a *single* particle is [14]

$$\sigma^2 = \int_{-\infty}^{\infty} x^2 p_s(x) dx = 2\Gamma(2H + 1). \quad (23)$$

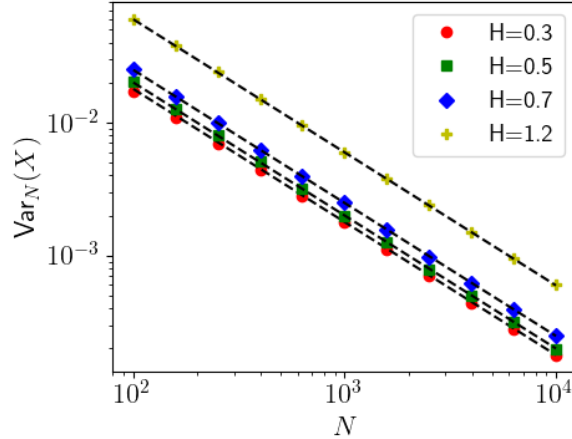


Figure 3: Variance of the center of mass X versus N , Eq. (24), for different values of H (see legend). Lines: theoretical predictions. Symbols: simulation results, where the simulation time is $t = 10^5$.

By virtue of additivity of the variance of independent random variables, the variance of the center of mass X is

$$\sigma_a^2 = \frac{2\Gamma(2H+1)}{N}, \quad (24)$$

which, in terms of the variance of the sum Σ , is equivalent to

$$\sigma_A^2 = \frac{N}{2\beta}, \quad \text{where} \quad \beta = \frac{1}{4\Gamma(2H+1)}. \quad (25)$$

Equations (24) and (25) hold for all $H > 0$. Fig. 3 shows a comparison of Eq. (24) with our numerical simulations.

4.1. $H \leq 1/2$: standard scaling

In this case the rate function $f(a)$ is given by Cramér's theorem, see e.g. Ref. [28]. Still, for completeness, we will calculate $f(a)$ from first principles. The starting point of this calculation is the exact one-particle position distribution $p_s(x)$ [14], described by Eq. (2). The joint steady-state distribution $P(x_1, x_2, \dots, x_N)$ of the positions of all particles can be obtained from the single-particle distribution:

$$P(x_1, x_2, \dots, x_N) = \left(\frac{r}{\sqrt{4\pi}} \right)^N \prod_{i=1}^N \int_0^\infty e^{-\frac{x_i^2}{4\tau^{2H}} - \tau} \tau^{-H} d\tau. \quad (26)$$

Then the distribution $P(a, N)$ can be written as

$$P(a, N) = \int_{-\infty}^{\infty} dx_1 \int_{-\infty}^{\infty} dx_2 \cdots \int_{-\infty}^{\infty} dx_N \prod_{i=1}^N p_s(x_i) \delta \left(\frac{1}{N} \sum_{i=1}^N x_i - a \right). \quad (27)$$

Using the exponential representation of the delta-function, we can rewrite this expression as

$$P(a, N) = \frac{N}{2\pi} \int_{-\infty}^{\infty} dk e^{-ikNa} \left[\int_{-\infty}^{\infty} dx e^{ikx} p_s(x) \right]^N. \quad (28)$$

The internal integral can be recast as follows:

$$F(k) \equiv \int_{-\infty}^{\infty} dx e^{ikx} p_s(x) = \int_0^{\infty} d\tau \tau^{-H} e^{-\tau} \int_{-\infty}^{\infty} dx e^{ikx - \frac{x^2}{4\tau^{2H}}}. \quad (29)$$

The integration over x is elementary, and we obtain

$$F(k) = \int_0^{\infty} d\tau e^{-\tau - k^2 \tau^{2H}}, \quad (30)$$

which leads to the exact expression

$$P(a, N) = \frac{N}{2\pi} \int_{-\infty}^{\infty} dk e^{-ikNa + N \ln F(k)}. \quad (31)$$

When $N \gg 1$ and $H < 1/2$ we can evaluate the integral in Eq. (31) by the saddle point method in the complex plane. The saddle-point equation is

$$\frac{F'(k)}{F(k)} = ia. \quad (32)$$

For $H < 1/2$ the saddle point k_* is purely imaginary: $k_* = i\kappa$, where κ is real, and Eq. (32) takes the form

$$a = 2\kappa \frac{\int_0^{\infty} d\tau \tau^{2H} e^{-\tau + \kappa^2 \tau^{2H}}}{\int_0^{\infty} d\tau e^{-\tau + \kappa^2 \tau^{2H}}}. \quad (33)$$

At a given a , Eq. (33) is an algebraic equation for κ . We are interested in the rate function $f(a, H)$, which determines $\mathcal{P}(a, N; H)$, up to subleading

pre-exponential factors, via the relation $-\ln P(a, N; H) \simeq N f(a, H)$, see Eq. (21). The saddle-point evaluation yields

$$f(a; H) = \kappa_*(a)a - \ln F[k_*(a)]. \quad (34)$$

This expression reproduces Cramér's theorem, see e.g. Ref. [28]. Equations (33) and (34) determine the rate function $f(a; H)$ in a parametric form, where κ plays the role of the parameter. Figure 4 shows plots of this rate function for $H = 1/8, 1/3$ and $1/2$.

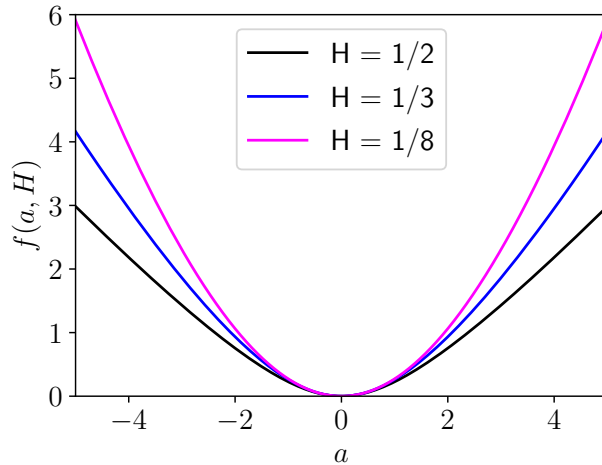


Figure 4: The rate function $f(a; H)$, see Eqs. (33) and (34), which describes the full statistics of the center of mass of the system for $H = 1/2, 1/3$, and $1/8$, see legend.

For $H = 1/2$ Eq. (30) simplifies to $F(k) = (1 + k^2)^{-1}$, and the relevant saddle point is

$$k = k_*(a) = i \left(\frac{1 - \sqrt{a^2 + 1}}{a} \right). \quad (35)$$

This yields the rate function in a simple analytic form,

$$f(a, 1/2) = \sqrt{a^2 + 1} + \ln \frac{2(\sqrt{a^2 + 1} - 1)}{a^2} - 1, \quad (36)$$

in agreement with Ref. [22]. In Fig. 4 the plot of $f(1, 1/2)$ is shown by the black curve.

Back to general H , the small- a region corresponds to the Gaussian fluctuations, which are dominated by the small- k region of the integral over

k in Eq. (31). Here we can, *for any* $H > 0$, Taylor-expand the exponent $\exp(-Dk^2\tau^{2H})$ in the integrand. The final result,

$$f(a \rightarrow 0, H) = \frac{a^2}{4\Gamma(2H + 1)}, \quad (37)$$

agrees with the expression (24) for the variance.

4.2. $H > 1/2$: anomalous scaling and phase transition

The contributions to the rate function $\phi(y)$ from the big jump, $O(A^{\frac{2}{2H+1}})$ [which is determined by the $|x| \gg 1$ tail of the single-particle distribution, see Eq. (3)], and from the Gaussian fluctuations, $O(A^2/N)$, are comparable for $A \sim N^{\frac{2H+1}{4H}}$. This simple estimate correctly predicts the anomalous scaling behavior (22) with the exponents

$$\mu = \frac{1}{2H} \quad \text{and} \quad \nu = \frac{2H+1}{4H}, \quad (38)$$

both of which are smaller than 1 once $H > 1/2$. The resulting rate function $\phi(y)$ has the following form [29]:

$$\phi(y) = \inf_{0 \leq z \leq y} \left[b(H) z^{\frac{2}{2H+1}} + \beta(H)(y - z)^2 \right], \quad (39)$$

where the coefficients

$$b(H) = \frac{2H+1}{2H} \left(\frac{H}{2} \right)^{\frac{1}{2H+1}} \quad \text{and} \quad \beta(H) = \frac{1}{4\Gamma(2H+1)} \quad (40)$$

follow from Eqs. (4) and (25), respectively. The first-order transition occurs at the point

$$y = y_c(H) = \frac{2H}{2H-1} \left[\frac{(2H-1)b(H)}{(2H+1)\beta(H)} \right]^{\frac{2H+1}{4H}}. \quad (41)$$

At $y < y_c$ one obtains the Gaussian asymptotic $\phi(y) = \beta(H)y^2$, while at $y \gg y_c$, $\phi(y)$ asymptotically approaches $b(H)y^{\frac{2}{2H+1}}$.

Figure 5 shows plots of the rate function $\phi(y)$ for three different values of $H > 1/2$ and the predicted critical point y_c in each case. One can see the two distinct behaviors of the rate function for $y < y_c(H)$ and $y > y_c(H)$.

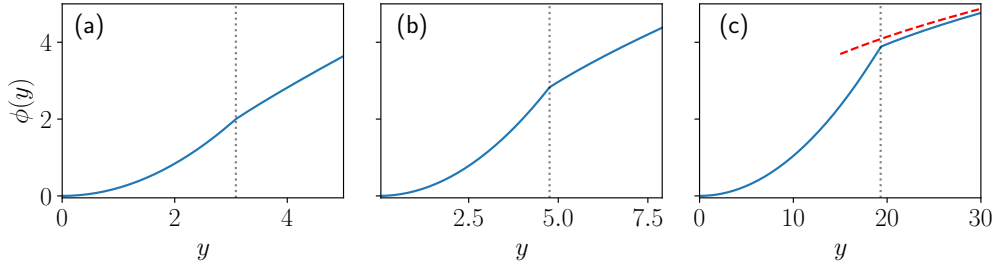


Figure 5: The anomalous rate function $\phi(y)$, see Eqs. (22) and (38), for $H = 2/3$ (a), $H = 1$ (b), and $H = 2$ (c). The critical point is described by Eq. (41) and is marked in all panels by a dotted line. The red dashed line in panel c shows the large- y asymptotic $b y^{\frac{2}{2H+1}}$.

5. Discussion

In this work we have analyzed collective statistical properties of a system of independently resetting scaled Brownian particles by focusing on the statistics of the system radius and of the center of mass.

Our first main result concerns the statistics of the system radius at the steady state. Since the steady-state position distribution of a single particle decays faster than any power law for all $H > 0$, the typical fluctuations that determine the moments of the distribution fall within the Gumbel universality class.

Our second main result deals with the COM statistics. As we have seen, these statistics exhibit a qualitative change of behavior at $H = 1/2$. For $H < 1/2$, the system is in a “condensed” state, which manifests itself in the conventional large-deviation statistics of the COM. In contrast, for $H > 1/2$ the system becomes susceptible to “big jumps” where a single particle can wander anomalously far from other particles and dominate the COM. This remarkable effect leads to an anomalous scaling for the COM and a nonanalyticity in the associated rate function which can be classified as a first-order dynamical phase transition. The transition between the two regimes occurs at $H = 1/2$.

Importantly, the collective statistical properties of the scaled Brownian particles, that we studied here, are ultimately determined by the properties of the single-particle steady state. This simplicity, however, is special to *noninteracting* particles. In many physical and biological systems anomalously diffusing particles experience strong interactions, crowding, or coupling

through nonlocal reset rules, and their collective fluctuations cannot be inferred from single-particle behavior alone [8, 33, 34, 22, 35, 2, 36, 37]. A first step in developing an adequate theoretical framework for interacting ensembles of anomalously diffusing particles under resetting has been made in Ref. [21] in hydrodynamic limit $N \rightarrow \infty$. The next step could be developing a fluctuating hydrodynamic theory that would be able to capture macroscopic fluctuations of these systems, such as the radius and the COM. For the standard Brownian motion of globally interacting particles with resetting fluctuating hydrodynamics was developed in Refs. [22, 35]. Its extension to anomalous diffusion such as the scaled Brownian motion therefore presents an interesting direction of future work.

Acknowledgments. We are grateful to Naftali R. Smith for valuable comments. B. M. was supported by the Israel Science Foundation (Grant No. 1579/25).

References

- [1] M. R. Evans, S. N. Majumdar, G. Schehr, Stochastic resetting and applications, *J. Phys. A: Math. Theor.* 53 (19) (2020) 193001.
- [2] R. Vatash, Y. Roichman, Many-body colloidal dynamics under stochastic resetting: Competing effects of particle interactions on the steady-state distribution, *Phys. Rev. Res.* 7 (3) (2025) L032020.
- [3] S. Gupta, A. M. Jayannavar, Stochastic resetting: A (very) brief review, *Frontiers in Physics* 10 (2022) 789097.
- [4] A. Kundu, S. Reuveni, Preface: stochastic resetting—theory and applications, *J. Phys. A: Math. Theor.* 57 (6) (2024) 060301.
- [5] S. Meir, T. D. Keidar, S. Reuveni, B. Hirshberg, First-passage approach to optimizing perturbations for improved training of machine learning models, *MLST* 6 (2) (2025) 025053.
- [6] J. R. Church, O. Blumer, T. D. Keidar, L. Ploutno, S. Reuveni, B. Hirshberg, Accelerating molecular dynamics through informed resetting, *J. Chem. Theory Comput.* 21 (2) (2025) 605–613.
- [7] M. R. Evans, S. N. Majumdar, Diffusion with stochastic resetting, *Phys. Rev. Lett.* 106 (16) (2011) 160601.

- [8] A. Nagar, S. Gupta, Stochastic resetting in interacting particle systems: A review, *J. Phys. A: Math. Theor.* 56 (28) (2023) 283001.
- [9] R. Metzler, J. Klafter, The random walk's guide to anomalous diffusion: a fractional dynamics approach, *Phys. Rep.* 339 (1) (2000) 1–77.
- [10] R. Metzler, J.-H. Jeon, A. G. Cherstvy, E. Barkai, Anomalous diffusion models and their properties: non-stationarity, non-ergodicity, and ageing at the centenary of single particle tracking, *Phys. Chem. Chem. Phys.* 16 (44) (2014) 24128–24164.
- [11] O. Vilk, E. Aghion, T. Avgar, C. Beta, O. Nagel, A. Sabri, R. Sarfati, D. K. Schwartz, M. Weiss, D. Krapf, et al., Unravelling the origins of anomalous diffusion: From molecules to migrating storks, *Phys. Rev. Res.* 4 (3) (2022) 033055.
- [12] A. Masó-Puigdellosas, D. Campos, V. Méndez, Transport properties and first-arrival statistics of random motion with stochastic reset times, *Phys. Rev. E* 99 (1) (2019) 012141.
- [13] A. Biswas, J. L. Dubbeldam, T. Sandev, A. Pal, A resetting particle embedded in a viscoelastic bath, *Chaos* 35 (3) (2025).
- [14] A. Bodrova, A. Chechkin, I. Sokolov, Scaled Brownian motion with renewal resetting., *Phys. Rev. E* 100 (1) (2019) 012120.
- [15] A. Bodrova, A. Chechkin, I. Sokolov, Nonrenewal resetting of scaled Brownian motion., *Phys. Rev. E* 100 (1) (2019) 012119.
- [16] W. Wang, A. G. Cherstvy, R. Metzler, I. M. Sokolov, Restoring ergodicity of stochastically reset anomalous-diffusion processes, *Phys. Rev. Res.* 4 (1) (2022) 013161.
- [17] Y. Liang, Q. Wei, W. Wang, A. G. Cherstvy, Ultraslow diffusion processes under stochastic resetting, *Phys. Fluids* 37 (3) (2025).
- [18] S. C. Lim, S. V. Muniandy, Self-similar Gaussian processes for modeling anomalous diffusion, *Phys. Rev. E* 66 (2) (2002) 021114.
- [19] J.-H. Jeon, A. V. Chechkin, R. Metzler, Scaled Brownian motion: a paradoxical process with a time dependent diffusivity for the description

of anomalous diffusion, *Phys. Chem. Chem. Phys.* 16 (30) (2014) 15811–15817.

- [20] H. Safdari, A. V. Chechkin, G. R. Jafari, R. Metzler, Aging scaled Brownian motion, *Phys. Rev. E* 91 (4) (2015) 042107.
- [21] B. Meerson, O. Vilk, Age-structured hydrodynamics of ensembles of anomalously diffusing particles with renewal resetting, arXiv:2512.1434 (2025).
- [22] O. Vilk, M. Assaf, B. Meerson, Fluctuations and first-passage properties of systems of Brownian particles with reset, *Phys. Rev. E* 106 (2) (2022) 024117.
- [23] R. A. Fisher, L. H. C. Tippett, Limiting forms of the frequency distribution of the largest or smallest member of a sample, in: *Mathematical proceedings of the Cambridge philosophical society*, Vol. 24, Cambridge University Press, 1928, pp. 180–190.
- [24] B. V. Gnedenko, Sur la distribution limite du terme maximum d'une série aléatoire, *Ann. Math.* 44 (3) (1943) 423–453.
- [25] E. J. Gumbel, *Statistics of Extremes*, Courier Corporation, 2004.
- [26] M. R. Leadbetter, G. Lindgren, H. Rootzén, *Extremes and related properties of random sequences and processes*, Springer Science & Business Media, 2012.
- [27] S. N. Majumdar, A. Pal, G. Schehr, Extreme value statistics of correlated random variables: A pedagogical review, *Phys. Rep.* 840 (43) (2020) 1–31.
- [28] V. V. Petrov, *Sums of independent random variables*, Vol. 82, Springer Science & Business Media, 2012.
- [29] S. V. Nagaev, Large deviations of sums of independent random variables, *Ann. Probab.* 7 (5) (1979) 745–789.
- [30] D. Denisov, A. B. Dieker, V. Shneer, Large deviations for random walks under subexponentiality: the big-jump domain, *Ann. Probab.* 36 (5) (2008) 1946–1991.

- [31] A. Vezzani, E. Barkai, R. Burioni, Single-big-jump principle in physical modeling, *Phys. Rev. E* 100 (1) (2019) 012108.
- [32] N. R. Smith, Anomalous scaling and first-order dynamical phase transition in large deviations of the Ornstein-Uhlenbeck process, *Phys. Rev. E* 105 (2022) 014120.
- [33] J. Berestycki, É. Brunet, J. Nolen, S. Penington, Brownian bees in the infinite swarm limit, *Ann. Probab.* 50 (6) (2022) 2133–2177.
- [34] J. Berestycki, É. Brunet, J. Nolen, S. Penington, A free boundary problem arising from branching Brownian motion with selection, *Trans. Am. Math. Soc.* 374 (09) (2021) 6269–6329.
- [35] M. Siboni, P. Sasorov, B. Meerson, Fluctuations of a swarm of Brownian bees, *Phys. Rev. E* 104 (5) (2021) 054131.
- [36] M. Biroli, H. Larralde, S. N. Majumdar, G. Schehr, Extreme statistics and spacing distribution in a Brownian gas correlated by resetting, *Phys. Rev. Lett.* 130 (20) (2023) 207101.
- [37] M. Biroli, S. N. Majumdar, G. Schehr, Resetting Dyson Brownian motion, *Phys. Rev. E* 112 (1) (2025) 014101.